APPLICABLE NONLINEAR ANALYSIS
Volume 1 (2024), No. 2, 170–186
https://doi.org/10.69829/apna-024-0102-ta03
Tulipa Opera Scholarum

A NUMERICAL ITERATION METHOD FOR THE CAUCHY PROBLEM IN LINEAR ELASTIC DYNAMICS

YAO SUN[1,*] AND MIN JIANG[1]

[1] *College of Science, Civil Aviation University of China, Tianjin, China*

Abstract. This paper investigates numerical solution methods for the Cauchy problem of the Navier equation on a connected domain. We utilize the measured Cauchy data on a portion of the domain boundary to invert the unknown Cauchy data on another portion of the boundary. First, we present the corresponding mathematical model, i.e. the Navier equation, and combine it with the known Cauchy data. Then, we discretize this mathematical model to obtain a corresponding ill-conditioned linear system of equations. We employ the pseudoinverse method, conjugate gradient method, and Tikhonov regularization method based on the Morozov discrepancy principle to solve this system of equations. The effectiveness of the algorithms is evaluated using spectral analysis. Next, we propose an improved Landweber iteration method. We first demonstrate the effectiveness of the algorithm using a filtering function and then analyze the errors of the algorithm to prove its stability and accuracy. Finally, we verify the stability and accuracy of the method through numerical experiments. Therefore, the proposed method is feasible and the numerical solutions obtained by this method can better approximate the true solution compared to several previous methods.

Keywords. Regularization methods; Navier equation; Landweber iterative, Cauchy problem.

1. Introduction

The elastic wave equation (Navier equation) has been widely applied in various fields of physics. Solving the Cauchy problem of the Navier equation is of utmost importance in non-destructive testing, imaging, and geophysical exploration techniques. By measuring data and solving the Cauchy problem, it is possible to infer information about the internal structure of materials, the location and shape of defects, and achieve material inspection and imaging. The research background of the Navier equation can be traced back to the early 19th century when scientists conducted in-depth studies on solid mechanics and wave phenomena. The development of the Navier equation aims to explain the propagation, reflection, refraction, and other phenomena of elastic waves in solids. It also seeks to predict and analyze wave phenomena such as seismic waves, sound waves, and vibrations. In [1, 2, 3],the stability of the Cauchy problem has been extensively examined. Marin et al. [4, 5] approached the Cauchy problem in linear elasticity by formulating it as a system of linear equations using the iteration BEM(Boundary Element Method). Numerous numerical methods have been introduced in the literature to solve the Cauchy problem in linear elasticity. The alternating iterative algorithm for the Cauchy problem in elasticity was presented in [6, 11] , while [7, 8, 9, 12]discuss other iterative methods. Marin [15] combined BEM with the Landweber method to solve the Cauchy problem in linear elasticity. Furthermore, [17]investigates the possibility of obtaining a stable approximate solution to the Cauchy problem in linear elasticity by utilizing the CGM (conjugate gradient method) in conjunction with the BEM. Other BEM-type methods can be found in [9, 18, 19, 21]. The FEM(Finite Element Method) is referenced in

*Corresponding author.
E-mail address: sunyao10@mails.jlu.edu.cn (Y. Sun), 15970683616@163.com (M.Jiang)
2020 Mathematics Subject Classification: Primary: 65F22; Secondary: 35Q74, 65N21.
Accepted: May 06, 2024.

[22, 23, 24] as a means of obtaining approximate solutions to boundary problems in partial differential equations. Fairweather and Karageorghis [26] have contributed to the literature on the MFS(Method of Fundamental Solutions) and related methods over the past three decades. It is worth noting that there is limited research available on the data completion problem in linear elastodynamics. However, in [27], the authors present a layer potential method for linear elastic dynamics. They conducted studies on convergence, provided stability estimates, and presented numerical examples to verify the efficiency of the proposed method. Additionally, in [35, 36], Chapko and coauthors discuss the boundary integral method in linear elastodynamics.

This paper is organized as follows. In Section 2, we introduce the mathematical model, which is the Navier equation, and incorporate it with the given Cauchy data. Subsequently, we discretize this mathematical model to obtain a corresponding ill-conditioned linear system of equations. In Section 3, we utilize the pseudoinverse method, conjugate gradient method, and Tikhonov regularization method based on the Morozov discrepancy principle to solve this system of equations. The effectiveness of these algorithms is evaluated using spectral analysis. Furthermore, in Section 3, we propose an improved Landweber iteration method. We first demonstrate the effectiveness of the algorithm using a filtering function and then analyze the errors of the algorithm to establish its stability and accuracy. In Section 3,We propose an improved Landweber iteration method. They first demonstrate the effectiveness of the algorithm using a filtering function and then analyze the errors of the algorithm to prove its stability and accuracy. In Section 4, we verify the stability and accuracy of the method through numerical experiments. The proposed method is proven to be feasible, and the numerical solutions obtained by this method exhibit closer approximation to the true solution compared to several previous methods.

2. Problem and Its Approximation

we consider a bounded connected domain $D \subset \mathbb{R}^2$ filled with an isotropic elastic medium of density ρ, and the boundary $\partial D = \Gamma \cup \Sigma$ of D is sufficiently smooth, where Γ and Σ are the known part and the unknown part of the boundary $\partial D$and $\Gamma \cap \Sigma = \emptyset$. Neglecting the body forces of the elastic medium itself, assuming the displacement field $\boldsymbol{u}$ corresponding to the stress tensor $\boldsymbol{\sigma}(\boldsymbol{u})$ in D satisfies the following Navier equations

$$\nabla \cdot \boldsymbol{\sigma}(\boldsymbol{u}) + \rho\omega^2 \boldsymbol{u} = 0, \quad \text{in } D. \tag{2.1}$$

where ω designates the frequency of vibration. For a linear isotropic elastic medium, the components of the stress tensor $\boldsymbol{\sigma}(\boldsymbol{u})$ be

$$\boldsymbol{\sigma}_{\imath\jmath} = \lambda\delta_{\imath\jmath}\boldsymbol{\varepsilon}_{\ell\ell} + 2\mu\boldsymbol{\varepsilon}_{\imath\jmath},\ \imath, \jmath = 1, 2,$$

with the strain tensor $\boldsymbol{\varepsilon}_{\imath\jmath}$ given by

$$\boldsymbol{\varepsilon}_{\imath\jmath} = \frac{1}{2}\left(\frac{\partial \boldsymbol{u}_\imath}{\partial \boldsymbol{x}_\jmath} + \frac{\partial \boldsymbol{u}_\jmath}{\partial \boldsymbol{x}_\imath}\right),$$

where $\delta_{\imath\jmath}$ is the Kronecker delta function, λ and μ, often referred to as the Lemé constants, and satisfy $\mu > 0$ and $\lambda + \mu > 0$.

2.1. **The Cauchy problem of Navier equations.**

Consider the following Cauchy problem: Where the displacement field $\boldsymbol{u}$ in D satisfies the following Navier equations

$$\mu\Delta\boldsymbol{u} + (\lambda + \mu)\nabla\nabla \cdot \boldsymbol{u} + \rho\omega^2\boldsymbol{u} = 0. \tag{2.2}$$

On the known boundary Γ, the displacement $\boldsymbol{u}$ satisfies the following boundary conditions:

- Dirichlet boundary condition

$$\boldsymbol{u} = \boldsymbol{f},\ \text{on } \Gamma. \tag{2.3}$$

- Neumann boundary condition

$$\boldsymbol{T}_n\boldsymbol{u} = \boldsymbol{t}, \text{ on } \Gamma. \tag{2.4}$$

Find the displacement field $\boldsymbol{u} \in C^2(D) \cap C(\bar{D})$, that is, determine the Cauchy data on Σ.

2.2. **Method of fundamental solutions.** The solution $\boldsymbol{u}$ of the Navier equations on a two dimensional plane can be decomposed into compressible and shear components through the Helmholtz decomposition

$$\boldsymbol{u} = \boldsymbol{u}_p + \boldsymbol{u}_s,$$

where $\boldsymbol{u}_p := (-1/k_p^2)\ grad\ \ div\ \ \boldsymbol{u}$ represents the the compressional part of $\boldsymbol{u}$, and $\boldsymbol{u}_s := (-1/k_s^2)$ $grad^{\perp}\ \ div^{\perp}\ \ \boldsymbol{u}$ represents the shear part of $\boldsymbol{u}$

$$grad^{\perp}\boldsymbol{u} := \left(-\frac{\partial \boldsymbol{u}}{\partial x_2}, \frac{\partial \boldsymbol{u}}{\partial x_1}\right)^{\top}; div^{\perp}\boldsymbol{u} := \frac{\partial \boldsymbol{u}_2}{\partial x_1} - \frac{\partial \boldsymbol{u}_1}{\partial x_2}.$$

the wavenumbers of compressional and shear waves k_p and k_s, respectively, are given by

$$k_s = \omega\sqrt{\frac{\rho}{\mu}}, k_p = \omega\sqrt{\frac{\rho}{\lambda + 2\mu}}.$$

There holds

$$\Delta\boldsymbol{u}_p + k_p^2\boldsymbol{u}_p = 0 \ \ and \ \ \Delta\boldsymbol{u}_s + k_s^2\boldsymbol{u}_s = 0$$

We know that the fundamental solution of the Helmholtz equation with a wavelength of k is given by the following

$$\Phi(k\,|\boldsymbol{x} - \boldsymbol{y}|) = \begin{cases} \frac{i}{4}H_0^{(1)}(k\,|\boldsymbol{x} - \boldsymbol{y}|), & \boldsymbol{x}, \boldsymbol{y} \in \mathbb{R}^2, \ \ \boldsymbol{x} \neq \boldsymbol{y}; \\ e^{ik|\boldsymbol{x}-\boldsymbol{y}|}/4\pi\,|\boldsymbol{x} - \boldsymbol{y}|, & \boldsymbol{x}, \boldsymbol{y} \in \mathbb{R}^3, \ \ \boldsymbol{x} \neq \boldsymbol{y}, \end{cases} \tag{2.5}$$

with $H_0^{(1)}$ be the Hankel function of the first kind of order zero. In this paper, we mainly consider the two-dimensional plane. From the Helmholtz decomposition, it can be inferred that $\Xi(\boldsymbol{x}, \boldsymbol{y})$ is the fundamental solution of the Navier equation on the two-dimensional plane. Its form can be determined as following

$$\Xi(\boldsymbol{x}, \boldsymbol{y}) = -\frac{i}{4}H_0^{(1)}(k_s r) - \frac{i}{4\rho\omega}\bigtriangledown_x \bigtriangledown_x^{\top}\left[H_0^{(1)}(k_s r) - H_0^{(1)}(k_p r)\right],$$

where $r = |\boldsymbol{x} - \boldsymbol{y}|$. The displacement field $\boldsymbol{u}$ can be approximate by discretisation as

$$\boldsymbol{u}(\boldsymbol{x}) \approx \boldsymbol{u}_N(\boldsymbol{x}) = \sum_{j=1}^{N} \boldsymbol{\Xi}(\boldsymbol{x}, \boldsymbol{y}_j)\begin{bmatrix} a_j \\ b_j \end{bmatrix}, \ \boldsymbol{x} \in D, \tag{2.6}$$

where $a_j, b_j, j = 1, 2, ..., N$, are the coefficients, $y_j \in \mathbb{R}^2 \setminus \overline{D}$ are the source points with the number N.

For a fixed point $\boldsymbol{x} \in \partial D$, $\boldsymbol{T}$ the traction operator defined on the boundary ∂D, is given by

$$(\boldsymbol{T}_n\boldsymbol{u})_\ell := \lambda\boldsymbol{n}_\ell\frac{\partial \boldsymbol{u}_\jmath}{\partial \boldsymbol{x}_\jmath} + \mu\boldsymbol{n}_\jmath\left(\frac{\partial \boldsymbol{u}_\ell}{\partial \boldsymbol{x}_\jmath} + \frac{\partial \boldsymbol{u}_\jmath}{\partial \boldsymbol{x}_\ell}\right), \ \ell = 1, 2,$$

where $\boldsymbol{n}$ is the unit outward normal vector. Combining the equation (2.6), we can get

$$\boldsymbol{t}(\boldsymbol{x}) \approx \boldsymbol{t}_N(\boldsymbol{x}) = \sum_{j=1}^{N} \boldsymbol{T}(\boldsymbol{x}, \boldsymbol{y}_j)\begin{bmatrix} a_j \\ b_j \end{bmatrix}. \tag{2.7}$$

The matrix $\boldsymbol{T}$ is given by

$$\boldsymbol{T}(\boldsymbol{x}, \boldsymbol{y}_j) = \begin{pmatrix} \boldsymbol{T}_{11}(\boldsymbol{x}, \boldsymbol{y}_j) & \boldsymbol{T}_{12}(\boldsymbol{x}, \boldsymbol{y}_j) \\ \boldsymbol{T}_{21}(\boldsymbol{x}, \boldsymbol{y}_j) & \boldsymbol{T}_{22}(\boldsymbol{x}, \boldsymbol{y}_j) \end{pmatrix},$$

whose elements are given by

$$\boldsymbol{T}_{11}(\boldsymbol{x},\boldsymbol{y}_j)=\left[(\lambda+2\mu)\frac{\partial \boldsymbol{U}_{11}(\boldsymbol{x},\boldsymbol{y}_j)}{\partial x_1}+\lambda\frac{\partial \boldsymbol{U}_{12}(\boldsymbol{x},\boldsymbol{y}_j)}{\partial x_2}\right]\boldsymbol{n}_1+\mu\left(\frac{\partial \boldsymbol{U}_{11}(\boldsymbol{x},\boldsymbol{y}_j)}{\partial x_2}+\frac{\partial \boldsymbol{U}_{12}(\boldsymbol{x},\boldsymbol{y}_j)}{\partial x_1}\right)\boldsymbol{n}_2,$$

$$\boldsymbol{T}_{12}(\boldsymbol{x},\boldsymbol{y}_j)=\left[(\lambda+2\mu)\frac{\partial \boldsymbol{U}_{12}(\boldsymbol{x},\boldsymbol{y}_j)}{\partial x_1}+\lambda\frac{\partial \boldsymbol{U}_{22}(\boldsymbol{x},\boldsymbol{y}_j)}{\partial x_2}\right]\boldsymbol{n}_1+\mu\left(\frac{\partial \boldsymbol{U}_{12}(\boldsymbol{x},\boldsymbol{y}_j)}{\partial x_2}+\frac{\partial \boldsymbol{U}_{22}(\boldsymbol{x},\boldsymbol{y}_j)}{\partial x_1}\right)\boldsymbol{n}_2,$$

$$\boldsymbol{T}_{21}(\boldsymbol{x},\boldsymbol{y}_j)=\mu\left(\frac{\partial \boldsymbol{U}_{11}(\boldsymbol{x},\boldsymbol{y}_j)}{\partial x_2}+\frac{\partial \boldsymbol{U}_{12}(\boldsymbol{x},\boldsymbol{y}_j)}{\partial x_1}\right)\boldsymbol{n}_1+\left[\lambda\frac{\partial \boldsymbol{U}_{11}(\boldsymbol{x},\boldsymbol{y}_j)}{\partial x_1}+(\lambda+2\mu)\frac{\partial \boldsymbol{U}_{12}(\boldsymbol{x},\boldsymbol{y}_j)}{\partial x_2}\right]\boldsymbol{n}_2,$$

$$\boldsymbol{T}_{22}(\boldsymbol{x},\boldsymbol{y}_j)=\mu\left(\frac{\partial \boldsymbol{U}_{12}(\boldsymbol{x},\boldsymbol{y}_j)}{\partial x_2}+\frac{\partial \boldsymbol{U}_{22}(\boldsymbol{x},\boldsymbol{y}_j)}{\partial x_1}\right)\boldsymbol{n}_1+\left[\lambda\frac{\partial \boldsymbol{U}_{12}(\boldsymbol{x},\boldsymbol{y}_j)}{\partial x_2}+(\lambda+2\mu)\frac{\partial \boldsymbol{U}_{22}(\boldsymbol{x},\boldsymbol{y}_j)}{\partial x_2}\right]\boldsymbol{n}_2.$$

where $\boldsymbol{U}$ is the fundamental solution of the Navier equation. The unknowns $\{a_j,b_j\}_{j=1}^N$ will be calculated by the collocation method. Generally, we choose M points $\{\boldsymbol{x}_i\}_{i=1}^M$ on the boundary Γ as the collocation points. Thus we will give a system about the unknowns, namely

$$\boldsymbol{A}\boldsymbol{\varphi}=\boldsymbol{b} \tag{2.8}$$

The matrix A has a large condition number due to the ill-posedness of the Cauchy problem, and therefore it is necessary to give a regularized stable solution. To solve in a stable way, we use the methods such as pseudo-inverse method, minimum solution method including the regularization parameter chosen by Morozov discrepancy principle, conjugate gradient method.

3. Several Numerical Solution Methods

In general, we consider the perturbed equation

$$\boldsymbol{A}\boldsymbol{\varphi}^\delta=\boldsymbol{b}^\delta \tag{3.1}$$

Here, $\boldsymbol{b}^\delta=(\boldsymbol{f}^\delta,\boldsymbol{t}^\delta)^\top$ is measured noisy data satisfying $\left\|\boldsymbol{b}^\delta-\boldsymbol{b}\right\|\le\delta\times\|\boldsymbol{b}\|=\sigma$ where δ is the noise level.

Theorem 3.1. *(Picard) Let $\boldsymbol{A}:\mathbb{F}\longrightarrow\mathbb{U}$ be a compact linear operator with singular system $(s_j,\boldsymbol{u}_j,\boldsymbol{v}_j)$. The equation of*

$$\boldsymbol{A}\boldsymbol{\varphi}=\boldsymbol{b}$$

is solvable if and only if $\boldsymbol{b}$ belongs to the orthogonal complement $\boldsymbol{b}\in\mathcal{N}(\boldsymbol{A}^*)^\perp$ and satisfies

$$\sum_{j\in J}\frac{1}{s_j^2}(\boldsymbol{b},\boldsymbol{v}_j)^2<\infty.$$

In this case a solution is given by

$$\boldsymbol{\varphi}=\sum_{j\in J}\frac{1}{s_j}(\boldsymbol{b},\boldsymbol{v}_j)\boldsymbol{u}_j.$$

Theorem 3.2. *Let $\boldsymbol{A}:\mathbb{F}\longrightarrow\mathbb{U}$ be an injective compact linear operator with singular system $(s_j,\boldsymbol{u}_j,\boldsymbol{v}_j)$, and let $q(\alpha,s):(0,\infty)\times(0,\|\boldsymbol{A}\|]\to\mathbb{R}$ satisfying the following conditions:*

1. For $\forall\alpha>0$ and $0<s<\|\boldsymbol{A}\|$, we have $|q(\alpha,s)|\le 1$.

2. There exists a function $c(\alpha)$ such that for $\forall\ 0<s<\|\boldsymbol{A}\|$, we have $|q(\alpha,s)|\le c(\alpha)s$.

3. For all $0<s<\|\boldsymbol{A}\|$, we have $\lim_{\alpha\to0}q(\alpha,s)=1$. $q(\alpha,s)$ is called a filtering function, and the following theorem holds:

1.Operator $R_\alpha:\mathbb{U}\longrightarrow\mathbb{F},\alpha>0$:

$$\boldsymbol{R}_\alpha\boldsymbol{b}=\sum_{j=1}^{\infty}\frac{q(\alpha,s_j)}{s_j}(\boldsymbol{b},\boldsymbol{v}_j)\boldsymbol{u}_j$$

is a regularization operator, and $\|\boldsymbol{R}_\alpha\|\le c(\alpha)$.

2.If we choose $\alpha = \alpha(\delta)$ such that $\alpha(\delta) \to 0$ as $\delta \to 0$ and $\delta c(\alpha(\delta)) \to 0$, then $\alpha = \alpha(\delta)$ is an admissible choice.

3.1. **Moore-Penrose generalized inverse matrix methods.** Using the Moore-Penrose pseudoinverse matrix provides a stable and reliable solution method for solving ill-conditioned systems of linear equations. The Moore-Penrose pseudoinverse matrix, denoted as $\boldsymbol{A}^{+}$, is a matrix that satisfies the following four conditions and has the same dimensions as $\boldsymbol{A}^{T}$ The Moore-Penrose pseudoinverse is a matrix A^{+} of the same dimensions as A^{T} satisfying four conditions:
(1) $\boldsymbol{A}\boldsymbol{A}^{+}\boldsymbol{A} = \boldsymbol{A}$,
(2) $\boldsymbol{A}^{+}\boldsymbol{A}\boldsymbol{A}^{+} = \boldsymbol{A}^{+}$,
(3) $\boldsymbol{A}\boldsymbol{A}^{+}$ is Hermitian,
(4) $\boldsymbol{A}^{+}\boldsymbol{A}$ is Hermitian.

The generalized inverse matrix of a matrix is not unique, and different generalized inverse matrices may lead to different solutions. Therefore, in practical applications, it may be necessary to choose an appropriate generalized inverse matrix based on the specific problem. One commonly used method for computing the Moore-Penrose generalized inverse matrix is the SVD (Singular Value Decomposition). In singular systems, the matrix $\boldsymbol{A}$ can be decomposed into the product of three matrices: $\boldsymbol{A} = \boldsymbol{U}\boldsymbol{S}\boldsymbol{V}^{T}$, where $\boldsymbol{U}$ and $\boldsymbol{V}$ are orthogonal matrices, and $\boldsymbol{S}$ is a diagonal matrix with its diagonal elements s_j known as singular values. When computing the generalized inverse matrix, $\boldsymbol{S}^{+}$ can be obtained by taking the inverse of $\boldsymbol{S}$ and then transposing it, where the nonzero singular values in $\boldsymbol{S}$ are reciprocated and placed on the diagonal. The solution to an ill-conditioned system of linear equations is represented as

$$\boldsymbol{A}^{+}\boldsymbol{b} = \boldsymbol{\varphi} = \sum_{j \in J} \frac{1}{s_j}(\boldsymbol{b}, \boldsymbol{v}_j)\boldsymbol{u}_j.$$

However, in practical computations, we may encounter singular values s_j that approach $\mathbf{0}$. If we introduce a perturbation $\boldsymbol{b}_{\delta}$ to $\boldsymbol{b}$, the perturbation of the solution $\boldsymbol{\varphi}^{\delta} = \sum_{j \in J} \frac{1}{s_j}(\boldsymbol{b}^{\delta}, \boldsymbol{v}_j)\boldsymbol{u}_j$ can deviate significantly from the true value, leading to numerical instability.

In order to avoid this situation, we use truncated singular value decomposition to approximate the generalized inverse matrix. We introduce a tolerance parameter, denoted as tol(tolerance), to control the truncation of singular values. The tolerance is a non-negative number that determines which singular values should be considered as non-zero when computing $\boldsymbol{S}^{+}$. Any value smaller than tol is treated as 0. We perform truncated singular value decomposition on the matrix $\boldsymbol{A}$, decomposing it into the product of three matrices:$\boldsymbol{A} = \boldsymbol{U}\boldsymbol{S}\boldsymbol{V}^{T}$, where $\boldsymbol{U}$ and $\boldsymbol{V}$ are orthogonal matrices, and $\boldsymbol{S}$ is a diagonal matrix. The approximate generalized inverse matrix of $\boldsymbol{A}$ can be represented as $\boldsymbol{A}^{+} = \boldsymbol{V}\boldsymbol{S}^{+}\boldsymbol{U}^{T}$. $\boldsymbol{S}^{+}$ is obtained by taking the reciprocals of the non-zero elements in $\boldsymbol{S}$ that are greater than tol, while considering the remaining elements as 0. Therefore, the solution to the perturbed equation (3.1) is given by $\boldsymbol{\varphi}^{\delta} = \boldsymbol{A}^{+} * \boldsymbol{b}^{\delta}$. Generally, a larger tolerance retains more singular values, resulting in a generalized inverse matrix that is closer to the inverse of the original matrix. From the perspective of the solution representation, it is as if a certain regularization filter has been introduced to the singular values, which can be seen as

$$\boldsymbol{\varphi} = \sum_{j \in J} \frac{q(tol, s_j)}{s_j}(\boldsymbol{b}, \boldsymbol{v}_j)\boldsymbol{u}_j.$$

where

$$q(tol, s_j) = \begin{cases} 1, & s_j^2 \geq tol, \\ 0, & s_j^2 < tol, \end{cases}$$

The condition $q(tol, s_j) \leq 1$is obviously satisfied. We choose

$$c(tol) = \frac{1}{\sqrt{tol}},$$

and when$s_j^2 \geq tol$, we have $c(tol)s_j \geq 1 = q(tol, s_j)$. Furthermore,

$$\lim_{tol \to 0} q(tol, s_j) = 1.$$

Clearly, $q(tol, s_j)$is a filtering function. According to Theorem3.2, the pseudoinverse method can be used to obtain a relatively stable numerical solution.

3.2. **Tikhonov regularization method.** We use the least squares method to transform the problem or equation (2.8) into the following equivalent problem of minimizing:

$$\min_{\varphi} \|\boldsymbol{A}\boldsymbol{\varphi} - \boldsymbol{b}\|_2^2 .$$

When solving the above minimization problem, we cannot guarantee the existence and uniqueness of the solution. Therefore, it is necessary to impose further restrictions on the minimizers to ensure their existence and uniqueness.

The idea of Tikhonov regularization is to solve this problem by adding a penalty term to the objective function. Specifically, we seek to minimize the Tikhonov functional:

$$J_\alpha(\boldsymbol{\varphi}) = \|\boldsymbol{A}\boldsymbol{\varphi} - \boldsymbol{b}\|_2^2 + \alpha \|\boldsymbol{\varphi}\|_2^2 , \tag{3.2}$$

where $\alpha > 0$ is called the regularization parameter.

Its solution is equivalent to the solution of the following equation:

$$(\boldsymbol{A}^*\boldsymbol{A} + \alpha \boldsymbol{I}) \varphi_\alpha = \boldsymbol{A}^*\boldsymbol{b}. \tag{3.3}$$

The solution to the problem can be expressed as the solution to the following equation:

$$\boldsymbol{\varphi}_\alpha = (\boldsymbol{A}^*\boldsymbol{A} + \alpha \boldsymbol{I})^{-1} \boldsymbol{A}^*\boldsymbol{b} = \boldsymbol{R}_\alpha \boldsymbol{b} \tag{3.4}$$

Since $\boldsymbol{A}$ is a compact operator, its singular system is given by $(s_j, \boldsymbol{u}_j, \boldsymbol{v}_j)$, where $\boldsymbol{A}\boldsymbol{\varphi}_j = s_j \boldsymbol{b}_j$, $\boldsymbol{A}^*\boldsymbol{b}_j = s_j \boldsymbol{\varphi}_j$. From $\boldsymbol{\varphi}_\alpha = (\boldsymbol{A}^*\boldsymbol{A} + \alpha\boldsymbol{I})^{-1}\boldsymbol{A}^*\boldsymbol{b}$, we have $(\boldsymbol{A}^*)^{-1}(\boldsymbol{A}^*\boldsymbol{A} + \alpha\boldsymbol{I})\boldsymbol{\varphi}_\alpha = \boldsymbol{b}$. Furthermore,

$$(\boldsymbol{A}^*)^{-1}(\boldsymbol{A}^*\boldsymbol{A} + \alpha\boldsymbol{I})\boldsymbol{\varphi}_j = \frac{\alpha + s_j^2}{s_j}\boldsymbol{b}; \quad (\boldsymbol{A}^*\boldsymbol{A} + \alpha\boldsymbol{I})^{-1}\boldsymbol{A}^*\boldsymbol{b}_j = \frac{\alpha + s_j^2}{s_j}\boldsymbol{\varphi}_j,$$

so the singular values of the operator $(\boldsymbol{A}^*)^{-1}(\boldsymbol{A}^*\boldsymbol{A} + \alpha\boldsymbol{I})$ are $\frac{\alpha + s_j^2}{s_j}$. Thus, the operator $\boldsymbol{R}_\alpha$ can be written in the following form:

$$\boldsymbol{R}_\alpha = \sum_{j=1}^{\infty} \frac{s_j}{\alpha + s_j^2}(\boldsymbol{b}, \boldsymbol{u}_j)\boldsymbol{v}_j = \sum_{j=1}^{\infty} \frac{q(\alpha, s_j)}{s_j}(\boldsymbol{b}, \boldsymbol{u}_j)\boldsymbol{v}_j,$$

where

$$q(\alpha, s_j) = \frac{s_j^2}{\alpha + s_j^2}.$$

It is clear from Theorem 3.2 that $q(tol, s_j)$ is a filter function. Therefore, the constructed operator $\boldsymbol{R}_\alpha$ is a regularization operator.

The regularization parameter is obtained by Morozov discrepancy principle. Morozov discrepancy principle is to choose the regularization parameter by finding the zeros of $G(\alpha) := \left\|\boldsymbol{A}\boldsymbol{\varphi}_\alpha^\delta - \boldsymbol{b}^\delta\right\|^2 - \sigma^2$. The zeros of $G(\alpha)$ are solved by Newton's method to obtain the regularization parameter as following:

- Initialize: $n = 0$, and take $\alpha_0 = \|\boldsymbol{A}\|^2 \delta / (\left\|\boldsymbol{b}^\delta\right\| - \sigma)$ as the initial value of the Newton iteration.

- For $n = 1, 2, ..., $ if $|\alpha_{n+1} - \alpha_n| > \varepsilon(\varepsilon \ll 1)$, continue the iteration

$$\begin{cases} \text{get } \boldsymbol{\varphi}_{\alpha_n}^{\delta} \text{ from } (\boldsymbol{A}^*\boldsymbol{A} + \alpha_n \boldsymbol{I})\boldsymbol{\varphi}_{\alpha_n}^{\delta} = \boldsymbol{A}^*\boldsymbol{b}^{\delta} \\ \text{get } \frac{d}{d\alpha}\boldsymbol{\varphi}_{\alpha_n}^{\delta} \text{ from } (\alpha_n \boldsymbol{I} + \boldsymbol{A}^*\boldsymbol{A})\frac{d}{d\alpha}\boldsymbol{\varphi}_{\alpha_n}^{\delta} = -\boldsymbol{\varphi}_{\alpha_n}^{\delta}. \\ G(\alpha_n) = \left\| \boldsymbol{A}\boldsymbol{\varphi}_{\alpha_n}^{\delta} - \boldsymbol{b}^{\delta} \right\|^2 - \sigma^2 \\ \nabla G(\alpha_n) = 2\alpha_n \left\| \boldsymbol{A}\frac{d}{d\alpha}\boldsymbol{\varphi}_{\alpha_n}^{\delta} \right\|^2 + 2\alpha_n^2 \left\| \frac{d}{d\alpha}\boldsymbol{\varphi}_{\alpha_n}^{\delta} \right\|^2, \\ \text{set } \alpha_{n+1} = \alpha_n - \frac{G(\alpha_n)}{\nabla G(\alpha_n)} \end{cases}$$

until $|\alpha_{n+1} - \alpha_n| < \varepsilon(\varepsilon \ll 1)$.

By introducing the regularization operator

$$\boldsymbol{R}_{\alpha} := (\alpha \boldsymbol{I} + \boldsymbol{A}^*\boldsymbol{A})^{-1}\boldsymbol{A}^*, \quad \alpha > 0,$$

we can achieve the regularized solution $\boldsymbol{\varphi}_{\alpha}^{\delta} = \boldsymbol{R}_{\alpha}\boldsymbol{b}^{\delta}$.

3.3. **Conjugate gradient method.** For the perturbation equation (3.1), we define function

$$f(\boldsymbol{\varphi}) := \left\| \boldsymbol{A}\boldsymbol{\varphi} - \boldsymbol{b}^{\delta} \right\|^2 = (\boldsymbol{A}\boldsymbol{\varphi} - \boldsymbol{b}^{\delta}, \boldsymbol{A}\boldsymbol{\varphi} - \boldsymbol{b}^{\delta}),$$

then $\nabla f(\boldsymbol{\varphi}) := 2\boldsymbol{A}^*(\boldsymbol{A}\boldsymbol{\varphi} - \boldsymbol{b}^{\delta})$. The steps of the conjugate gradient algorithm are as follows:

- Initialize: $\boldsymbol{\varphi}_0^{\delta} = \boldsymbol{\varphi}^*$, $\boldsymbol{d}_0 = \boldsymbol{b}^{\delta} - \boldsymbol{A}\boldsymbol{\varphi}_0^{\delta}$, $\boldsymbol{p}_1 = \boldsymbol{s}_0 = \boldsymbol{A}^*\boldsymbol{d}_0$, where $\boldsymbol{\varphi}^*$ is the initial guess;
- For $k = 1, 2, ..., 200$. If $s_{k-1} \neq 0$, compute

$$\begin{cases} \boldsymbol{q}_k = \boldsymbol{A}\boldsymbol{p}_k, \\ \alpha_k = \|\boldsymbol{s}_{k-1}\|^2 / \|\boldsymbol{q}_k\|^2, \\ \boldsymbol{\varphi}_k^{\delta} = \boldsymbol{\varphi}_{k-1}^{\delta} + \alpha_k \boldsymbol{p}_k, \\ \boldsymbol{d}_k = \boldsymbol{d}_{k-1} - \alpha_k \boldsymbol{p}_k, \\ \boldsymbol{s}_k = \boldsymbol{A}^*\boldsymbol{d}_k, \\ \beta_k = \|\boldsymbol{s}_k\|^2 / \|\boldsymbol{s}_{k-1}\|^2, \\ \boldsymbol{p}_{k-1} = \boldsymbol{s}_k + \beta_k \boldsymbol{p}_k, \end{cases}$$

until $\boldsymbol{s}_{k-1} = \boldsymbol{0}$. The iteration converges only when $\boldsymbol{A}$ is a positive definite matrix.

4. Landweber Iteration Method

The solution to the equation (2.8) is equivalent to the solution of the following linear system:

$$\boldsymbol{\varphi} = \boldsymbol{\varphi} + \omega \boldsymbol{A}^*(\boldsymbol{b} - \boldsymbol{A}\boldsymbol{\varphi}) \tag{4.1}$$

Therefore, we introduce the following Landweber iteration scheme:

$$\boldsymbol{\varphi}_k = \boldsymbol{\varphi}_{k-1} + \omega \boldsymbol{A}^*(\boldsymbol{b} - \boldsymbol{A}\boldsymbol{\varphi}_{k-1}) \tag{4.2}$$

4.1. **The effectiveness of the landweber iterative method.** We know that

$$\boldsymbol{\varphi}_k = (\boldsymbol{I} - \omega \boldsymbol{A}^*\boldsymbol{A})\boldsymbol{\varphi}_{k-1} + \omega \boldsymbol{A}^*\boldsymbol{b}^{\delta},$$

and by recursion, we have

$$\boldsymbol{\varphi}_k = \omega \sum_{k=0}^{k-1} (\boldsymbol{I} - \omega \boldsymbol{A}^*\boldsymbol{A})^j \boldsymbol{A}^*\boldsymbol{b}^{\delta} + (\boldsymbol{I} - \omega \boldsymbol{A}^*\boldsymbol{A})^k \boldsymbol{\varphi}_0.$$

Usually, we take the initial value of the iteration as $\boldsymbol{\varphi}_0 = \boldsymbol{0}$. We define the operatoras $\boldsymbol{R}_K$ as

$$\boldsymbol{R}_K := \omega \sum_{k=0}^{K-1} (\boldsymbol{I} - \omega \boldsymbol{A}^*\boldsymbol{A})^k \boldsymbol{A}^*.$$

The expression of $\boldsymbol{\varphi}_K$ can be represented as $\boldsymbol{\varphi}_K = \boldsymbol{R}_K \boldsymbol{b}^\delta$. Expanding $\boldsymbol{R}_k$ using the singular system $(s_j, \boldsymbol{u}_j, \boldsymbol{v}_j)$ of the compact operator $\boldsymbol{A}$, we have the following expression for $\boldsymbol{R}_K$:

$$\begin{aligned}\boldsymbol{R}_k : \quad &= \omega \sum_{j=1}^{\infty} \sum_{k=0}^{K-1} (1-\omega s_j^2)^k (\boldsymbol{b}, \boldsymbol{v}_j) s_j \boldsymbol{u}_j \\ &= \sum_{j=1}^{\infty} \frac{1}{s_j} [1-(1-\omega s_j^2)^K] (\boldsymbol{b}, \boldsymbol{v}_j) \boldsymbol{u}_j \\ &= \sum_{j=1}^{\infty} \frac{q(K, s_j)}{s_j} (\boldsymbol{b}, \boldsymbol{v}_j) \boldsymbol{u}_j\end{aligned}$$

We take $\alpha = 1/K$, and when $0 < \omega \leq 1/\left\|\boldsymbol{A}\right\|^2$, the inequality $p(K, s_j) = q(\alpha, s_j) = 1-(1-\omega s_j^2)^{1/\alpha} \leq 1$ holds. Using the Bernoulli inequality, we can obtain:

$$q(\alpha, s_j) = 1-(1-\omega s_j^2)^{1/\alpha} \leq 1-(1-\frac{\omega s_j^2}{\alpha}) = \frac{\omega s_j^2}{\alpha},$$

Therefore, we can take $c(\alpha) = \sqrt{\frac{\omega}{\alpha}}?$, then $q(\alpha, s_j) \leq \sqrt{q(\alpha, s_j)} \leq c(\alpha) s_j?$. Since $1-\omega s_j^2 < 1$, we have:

$$\lim_{\alpha \to 0} q(\alpha, s_j) = \lim_{K \to \infty} p(K, s_j) = \lim_{K \to \infty} (1-(1-\omega s_j^2)^K) = 1.$$

Therefore, when $0 < \omega \leq 1/\left\|\boldsymbol{A}\right\|^2$, the constructed operator is a regular operator, and stable numerical solutions can be obtained through iteration.

4.2. **Convergence of the Landweber iteration method.** Assuming $\boldsymbol{\varphi}^+ = \boldsymbol{A}^+ \boldsymbol{b}^\delta$, where $\boldsymbol{\varphi}^+$ is the least squares solution of $\boldsymbol{A}\boldsymbol{\varphi} = \boldsymbol{b}^\delta$. Let $\mathcal{D}(\boldsymbol{A}^+)$ be the range of $\boldsymbol{A}^+$. Due to errors in the measured Cauchy data $\boldsymbol{b}^\delta$, when the value of $\boldsymbol{b}^\delta$ is not in $\mathcal{D}(\boldsymbol{A}^+)$, the iteration cannot converge to the true solution. We have the following theorem.

Theorem 4.1. *Let $\{\boldsymbol{\varphi}_k\}$ be the sequence of iterates generated by the iterative scheme (4.2). As $k \to \infty$, if $\boldsymbol{b}^\delta \in \mathcal{D}(\boldsymbol{A}^+)$, then $\boldsymbol{\varphi}_k \to \boldsymbol{A}^+ \boldsymbol{b}^\delta$. If $\boldsymbol{b}^\delta \notin \mathcal{D}(\boldsymbol{A}^+)$, then $\boldsymbol{\varphi}_k \to \infty$.*

Proof. Assuming $\boldsymbol{b}^\delta \in \mathcal{D}(\boldsymbol{A}^+)$, for $\boldsymbol{\varphi}^+ = \boldsymbol{A}^+ \boldsymbol{b}^\delta$, we have $\boldsymbol{A}^* \boldsymbol{b}^\delta = \boldsymbol{A}^* \boldsymbol{A} \boldsymbol{\varphi}^+$. Therefore,

$$\boldsymbol{\varphi}^+ - \boldsymbol{\varphi}_k = \boldsymbol{\varphi}^+ - \omega \boldsymbol{A}^* \boldsymbol{A} \sum_{j=0}^{k-1} (\boldsymbol{I} - \omega \boldsymbol{A}^* \boldsymbol{A})^j \boldsymbol{\varphi}^+.$$

Since the following equation holds:

$$\omega \boldsymbol{A}^* \boldsymbol{A} \sum_{j=0}^{k-1} (\boldsymbol{I} - \omega \boldsymbol{A}^* \boldsymbol{A})^j = \boldsymbol{I} - (\boldsymbol{I} - \omega \boldsymbol{A}^* \boldsymbol{A})^k,$$

we can deduce that

$$\boldsymbol{\varphi}^+ - \boldsymbol{\varphi}_k = (\boldsymbol{I} - \omega \boldsymbol{A}^* \boldsymbol{A})^k \boldsymbol{\varphi}^+.$$

Furthermore, $0 < \|\omega \boldsymbol{A}^* \boldsymbol{A}\| \leq \omega \left\|\boldsymbol{A}\right\|^2 \leq 1$, so $|\boldsymbol{I} - \omega \boldsymbol{A}^* \boldsymbol{A}| < 1$,

$$\lim_{k \to \infty} \left\|\boldsymbol{\varphi}^+ - \boldsymbol{\varphi}_k\right\| = \lim_{k \to \infty} \left\|(\boldsymbol{I} - \omega \boldsymbol{A}^* \boldsymbol{A})^k \boldsymbol{\varphi}^+\right\| \leq \lim_{k \to \infty} \left|(\boldsymbol{I} - \omega \boldsymbol{A}^* \boldsymbol{A})^k\right| \left\|\boldsymbol{\varphi}^+\right\| = 0,$$

which implies that $\boldsymbol{\varphi}_k \to \boldsymbol{A}^+ \boldsymbol{b}^\delta$.

Assuming $\boldsymbol{b}^\delta \notin \mathcal{D}(\boldsymbol{A}^+)$, we will use a proof by contradiction. Suppose that $\{\boldsymbol{\varphi}_k\}$ is bounded in the Hilbert space, then there exists a convergent subsequence $\{\boldsymbol{\varphi}_{k_n}\}$. Since the operator A has weak convergence, we have $\boldsymbol{A}\boldsymbol{\varphi}_{k_n} = \boldsymbol{A}\boldsymbol{\varphi}$. So, $\boldsymbol{A}\boldsymbol{\varphi}_{k_n} = \boldsymbol{A}\boldsymbol{\varphi} \to Q\boldsymbol{b}^\delta$, where $Q = Q|_{\mathcal{D}(\boldsymbol{A}^+)}$. Therefore, $\boldsymbol{b}^\delta \in \mathcal{D}(\boldsymbol{A}^+)$. By contrapositive, if $\boldsymbol{b}^\delta \notin \mathcal{D}(\boldsymbol{A}^+)$, then $\{\boldsymbol{\varphi}_k\}$ is unbounded. □

When $\boldsymbol{b}^\delta \notin \mathcal{D}(\boldsymbol{A}^+)$, the Landweber iteration does not converge. For the case of non-convergence, we have the following theorem.

Theorem 4.2. *If* $\|\boldsymbol{b} - \boldsymbol{b}_\delta\| \leq \delta * \|\boldsymbol{b}_\delta\| = \sigma, \boldsymbol{b}_\delta \notin \mathcal{D}(\boldsymbol{A}^+)$, *then* $\left\|\boldsymbol{\varphi}_k - \boldsymbol{\varphi}_k^\delta\right\| \leq \sqrt{k\omega}\sigma, k \geq 0$.

Proof.

$$\boldsymbol{\varphi}_k - \boldsymbol{\varphi}_k^\delta = \omega \sum_{j=0}^{k-1} (\boldsymbol{I} - \omega \boldsymbol{A}^*\boldsymbol{A})^j \boldsymbol{A}^*(\boldsymbol{b} - \boldsymbol{b}_\delta) := \boldsymbol{R}_k(\boldsymbol{b} - \boldsymbol{b}_\delta),$$

and

$$\|\boldsymbol{R}_k\|^2 = \|\boldsymbol{R}_k\boldsymbol{R}_k^*\| = \omega \left\| \sum_{j=0}^{k-1} (\boldsymbol{I} - \omega\boldsymbol{A}^*\boldsymbol{A})^j (\boldsymbol{I} - (\boldsymbol{I} - \omega\boldsymbol{A}^*\boldsymbol{A})^k) \right\| \leq \omega \left\| \sum_{j=0}^{k-1} (\boldsymbol{I} - \omega\boldsymbol{A}^*\boldsymbol{A})^j \right\|.$$

Therefor

$$\|\omega\boldsymbol{A}^*\boldsymbol{A}\| \leq 1; \|\boldsymbol{I} - \omega\boldsymbol{A}^*\boldsymbol{A}\| \leq 1,$$

So

$$\left\|\boldsymbol{\varphi}_k - \boldsymbol{\varphi}_k^\delta\right\| \leq \sqrt{k\omega}\sigma.$$

□

Because

$$\left\|\boldsymbol{\varphi}^+ - \boldsymbol{\varphi}_k\right\| \leq \left\|\boldsymbol{\varphi}^+ - \boldsymbol{\varphi}_k\right\| + \left\|\boldsymbol{\varphi}_k - \boldsymbol{\varphi}_k^\delta\right\|,$$

when the error level σ is small and the number of iterations k is small, the data error $\left\|\boldsymbol{\varphi}_k - \boldsymbol{\varphi}_k^\delta\right\| \ll 1$ can be ignored. However, as k becomes larger, the error increases, leading to the phenomenon of semi-convergence. Therefore, choosing an appropriate iteration index k plays a role as a regularization parameter.

4.3. **Improved Landweber iteration.** Through the above proof, we know that when $\boldsymbol{b}^\delta \in \mathcal{D}(\boldsymbol{A}^+)$, the Landweber iteration converges to $\boldsymbol{A}^+\boldsymbol{b}^\delta$. However, when $\boldsymbol{b}^\delta \notin \mathcal{D}(\boldsymbol{A}^+)$, the iteration error first decreases and then increases, which means that the iteration initially converges and then diverges. In both cases, the choice of the number of iterations becomes crucial. It plays a role similar to the regularization parameter mentioned earlier. Only by selecting an appropriate number of iterations can we approach the true solution effectively.

For the first case, we can choose the initial value of the iteration as the regularized solution obtained by the Morozov discrepancy principle: $\boldsymbol{\varphi}_\alpha(\alpha\boldsymbol{I} + \boldsymbol{A}^*\boldsymbol{A})^{-1}\boldsymbol{A}^*\boldsymbol{b}^\delta$. The number of iterations can be set as the ceiling value of the reciprocal of the regularization parameter, i.e., $n = \lceil \alpha^{-1} \rceil$.

For the second case, we have the following theorem:

Lemma 4.3. *Suppose* $\boldsymbol{b}^\delta \notin \mathcal{D}(\boldsymbol{A}^+)$, $b \in \mathcal{R}(A)$, *and* $\boldsymbol{\varphi} \in \mathcal{D}(\boldsymbol{A})$ *satisfies* $\boldsymbol{A}\boldsymbol{\varphi} = \boldsymbol{b}$. *If* $\left|\boldsymbol{A}\boldsymbol{\varphi}_k^\delta - \boldsymbol{b}^\delta\right| \geq 2\delta$, *then* $\boldsymbol{\varphi}_{k+1}^\delta$ *provides a better approximation to the true solution* $\boldsymbol{\varphi}^+$ *than* $\boldsymbol{\varphi}_k^\delta$.

In this paper, we determine whether $\boldsymbol{b}^\delta$ belongs to $\mathcal{D}(\boldsymbol{A}^+)$ by comparing the differences between the numerical solutions obtained by two different iteration methods. Let's assume the numerical solutions obtained by these two methods are $\boldsymbol{\varphi}_n^\delta$ and $\boldsymbol{\psi}_m^\delta$. The main difference between the two methods lies in the number of iterations. If $\boldsymbol{b}^\delta \in \mathcal{D}(\boldsymbol{A}^+)$, the iterative values obtained by both methods will be close to each other. In this case, we choose $\boldsymbol{\varphi}_n^\delta$ as the numerical solution. On the other hand, when $\boldsymbol{b}^\delta \notin \mathcal{D}(\boldsymbol{A}^+)$, the former iteration diverges, while the latter converges better to the true value, resulting in a larger difference between them. In this case, we select $\boldsymbol{\psi}_m^\delta$ as the numerical solution. We use the error level δ

as a criterion to determine whether $\boldsymbol{b}^\delta$ belongs to $\mathcal{D}(\boldsymbol{A}^+)$. If $\left\|\boldsymbol{\varphi}_n^\delta - \boldsymbol{\psi}_m^\delta\right\| < \delta \times \|\boldsymbol{b}\| = \sigma$, we consider $\boldsymbol{b}^\delta \in \mathcal{D}(\boldsymbol{A}^+)$, and we choose $\boldsymbol{\varphi}_n^\delta$ as the numerical solution. If $\left\|\boldsymbol{\varphi}_n^\delta - \boldsymbol{\psi}_m^\delta\right\| \geq \delta \times \|\boldsymbol{b}\| = \sigma$, we consider $\boldsymbol{b}^\delta \notin \mathcal{D}(\boldsymbol{A}^+)$, and we choose $\boldsymbol{\psi}_m^\delta$ as the numerical solution. Therefore, we have the following improved Landweber iteration method.

The steps for the improved Landweber iteration method are as follows:

• Initialization: The regularization parameter α is obtained from the Morozov discrepancy principle. Set $\omega = 1/(2\|\boldsymbol{A}\|^2)$, $\boldsymbol{\varphi}_0 = \boldsymbol{\psi}_0 = \boldsymbol{\varphi}_\alpha(\alpha \boldsymbol{I} + \boldsymbol{A}^*\boldsymbol{A})^{-1}\boldsymbol{A}^*\boldsymbol{b}^\delta$ as the initial values, and the number of iterations $n = \lceil \alpha^{-1} \rceil$.

• For $k = 1, 2, ..., n$.

$$\boldsymbol{\varphi}_k^\delta = \boldsymbol{\varphi}_{k-1}^\delta + \omega \boldsymbol{A}^*(\boldsymbol{b}^\delta - \boldsymbol{A}\boldsymbol{\varphi}_{k-1}^\delta)$$

Obtain $\boldsymbol{\varphi}_n^\delta$.

• Then for $k = 1, 2, ...$

$$\boldsymbol{\psi}_k^\delta = \boldsymbol{\psi}_{k-1}^\delta + \omega \boldsymbol{A}^*(\boldsymbol{b}^\delta - \boldsymbol{A}\boldsymbol{\psi}_{k-1}^\delta)$$

• Stop the iteration when $\left\|\boldsymbol{A}\boldsymbol{\psi}_k^\delta - \boldsymbol{b}^\delta\right\| < 2\sigma$, and obtain $\boldsymbol{\psi}_m^\delta$.

• If $\left\|\boldsymbol{\varphi}_n^\delta - \boldsymbol{\psi}_m^\delta\right\| < \delta \times \|\boldsymbol{b}\| = \sigma$, then the numerical solution is $\boldsymbol{\varphi}_n^\delta$. If $\left\|\boldsymbol{\varphi}_n^\delta - \boldsymbol{\psi}_m^\delta\right\| \geq \delta \times \|\boldsymbol{b}\| = \sigma$, then the numerical solution is $\boldsymbol{\psi}_m^\delta$

The algorithm defined in the document can be represented by the operator R with the following expression:

$$\begin{aligned} R: \quad &= \sum_{j=1}^{\infty} \frac{1 - (1 - \omega s_j^2)^k \frac{\alpha}{\alpha + s_j^2}}{s_j} (\boldsymbol{b}, \boldsymbol{v}_j)\boldsymbol{u}_j \\ &= \sum_{j=1}^{\infty} \frac{q(1/k, \alpha, s_j)}{s_j} (\boldsymbol{b}, \boldsymbol{v}_j)\boldsymbol{u}_j. \end{aligned}$$

We obtain the function:

$$q(1/k, \alpha, s) = 1 - (1 - \omega s^2)^k \frac{\alpha}{\alpha + s^2},$$

where k depends on α, so the function $q(1/k, \alpha, s)$ actually has only two variables, and $1/k < \alpha$. It can be proven that this function is a filtering function.

Proof. Since $1/k > 0$, $\alpha > 0$, and $1 - \omega s^2 < 1$, we have:

$$q(1/k, \alpha, s) \leq 1 - (1 - \omega s^2)^k \leq 1,$$

Using the Bernoulli inequality, we can deduce:

$$\begin{aligned} q(1/k, \alpha, s_j) \quad &= 1 - (1 - \omega s^2)^k \frac{\alpha}{\alpha + s^2} \\ &\leq 1 - (1 - k\omega s^2) \frac{\alpha}{\alpha + s^2} \\ &= \frac{s^2}{\alpha + s^2} + k\omega s^2 \frac{\alpha}{\alpha + s^2}, \end{aligned}$$

Therefore, we have the following inequality:

$$q(1/k, \alpha, s) \leq \sqrt{q(1/k, \alpha, s)} = s\sqrt{\frac{1}{\alpha + s^2} s + k\omega} \leq s\frac{1}{\sqrt{\alpha + s^2}} + s\sqrt{k\omega},$$

We can choose $c(1/k,\alpha) = 1/\sqrt{\alpha + s^2} + \sqrt{k\omega}$, such that $q(1/k,\alpha,s) \leq sc(1/k,\alpha)$ holds. Furthermore,

$$\lim_{1/k,\alpha\to 0} q(1/k,\alpha,s) = 1$$

is obviously true. According to Theorem 3.2, we know that the constructed algorithm is a regularization algorithm □

4.4. **Error analysis.** When $\boldsymbol{b}^\delta \in \mathcal{D}(\boldsymbol{A}^+)$, from equation (4.2), we know that:

$$\boldsymbol{\varphi}_k^\delta = (\boldsymbol{I} - \omega \boldsymbol{A}^*\mathbf{A})\boldsymbol{\varphi}_{k-1}^\delta + \omega \boldsymbol{A}^*\boldsymbol{b}^\delta,$$

By recursion, we have:

$$\begin{aligned}\boldsymbol{\varphi}_n^\delta &= (\boldsymbol{I} - \omega \boldsymbol{A}^*\boldsymbol{A})\boldsymbol{\varphi}_{n-1}^\delta + \omega \boldsymbol{A}^*\boldsymbol{b}^\delta \\ &= \omega \sum_{j=0}^{n-1} (\boldsymbol{I} - \omega \boldsymbol{A}^*\boldsymbol{A})^j \boldsymbol{A}^*\boldsymbol{b}^\delta + (\boldsymbol{I} - \omega \boldsymbol{A}^*\boldsymbol{A})^n \boldsymbol{\varphi}_0.\end{aligned}$$

Also, $\boldsymbol{b}^\delta \in \mathcal{D}(\boldsymbol{A}^+)$, for $\boldsymbol{\varphi}^+ = \boldsymbol{A}^+\boldsymbol{b}^\delta$, we have $\boldsymbol{A}^*\boldsymbol{b}^\delta = \boldsymbol{A}^*\boldsymbol{A}\boldsymbol{\varphi}^+$. Therefore, $\boldsymbol{A}^*\boldsymbol{b}^\delta = \boldsymbol{A}^*\boldsymbol{A}\boldsymbol{\varphi}^+$ We also have the identity:

$$\omega \boldsymbol{A}^*\boldsymbol{A} \sum_{j=0}^{n-1} (\boldsymbol{I} - \omega \boldsymbol{A}^*\boldsymbol{A})^j = \boldsymbol{I} - (\boldsymbol{I} - \omega \boldsymbol{A}^*\boldsymbol{A})^n,$$

Thus,

$$\boldsymbol{\varphi}^+ - \boldsymbol{\varphi}_n^\delta = (\boldsymbol{I} - \omega \boldsymbol{A}^*\boldsymbol{A})^n \boldsymbol{\varphi}^+ - (\boldsymbol{I} - \omega \boldsymbol{A}^*\boldsymbol{A})^n \boldsymbol{\varphi}_\alpha,$$

$$\begin{aligned}\left\|\boldsymbol{\varphi}^+ - \boldsymbol{\varphi}_n^\delta\right\| &= \left\|(\boldsymbol{I} - \omega \boldsymbol{A}^*\boldsymbol{A})^n (\boldsymbol{\varphi}^+ - \boldsymbol{\varphi}_\alpha)\right\| \\ &\leq \left|(\boldsymbol{I} - \omega \boldsymbol{A}^*\boldsymbol{A})^n\right| \left\|\boldsymbol{\varphi}^+ - \boldsymbol{\varphi}_\alpha\right\|.\end{aligned}$$

Also, $0 < \|\omega \boldsymbol{A}^*\boldsymbol{A}\| \leq \omega \|\boldsymbol{A}\|^2 \leq 1$, hence $|(\boldsymbol{I} - \omega \boldsymbol{A}^*\boldsymbol{A})^n| < 1$. Therefore, $\left\|\boldsymbol{\varphi}^+ - \boldsymbol{\varphi}_n^\delta\right\| < \|\boldsymbol{\varphi}^+ - \boldsymbol{\varphi}_\alpha\|$. The improved iterative method can approximate the true value better than the minimum norm solution method. If we take $\boldsymbol{\varphi}_0 = \mathbf{0}$ as the initial value of the iteration, similarly, we can see that the generated error is $\left\|\boldsymbol{\varphi}^+ - \boldsymbol{\varphi}_n^\delta\right\| = |(\boldsymbol{I} - \omega \boldsymbol{A}^*\boldsymbol{A})^n| \|\boldsymbol{\varphi}^+\|$. Generally, $\boldsymbol{\varphi}_\alpha$ is closer to the true value than 0, so usually $\|\boldsymbol{\varphi}^+ - \boldsymbol{\varphi}_\alpha\| < \|\boldsymbol{\varphi}^+\|$, which means that the improved Landweber iteration method can usually approximate the true value better than the Landweber iteration method and the minimum norm method.

5. Numerical Examples

In this section, we report some examples to demonstrate the effectiveness of our algorithm.

Example 5.1. In this example, the exact solution is given by

$$\boldsymbol{u}(\boldsymbol{x}) = \boldsymbol{\Xi}(\boldsymbol{x}, \boldsymbol{y}_0)\boldsymbol{p},$$

with $\boldsymbol{y}_0 = (10, 10)$, $\boldsymbol{p} = (1, 0)^\top$. The known part boundary is given by $\Gamma = (\cos t, \sin t)$, $t \in [0, \pi]$, and the missing part of the boundary is $\Sigma = (\cos t, 0.5 \sin t)$, $t \in (\pi, 2\pi)$. We choose $\partial B = (5 \cos t, 5 \sin t)$, $t \in [0, \pi]$, and investigate the case $\omega = 3$, $\lambda = \mu = 1$.

We choose the discrete points $N = 160$ of boundary Γ and the discrete points $M = 80$ on virtual boundary. Figure 1 shows the solution domain, Figure 2 shows the numerical solutions obtained by different methods and the exact solution for Example 2 when the noise level is $\delta = 0.1 \|\boldsymbol{b}\|$. It can be observed that the improved Landweber iteration method provides numerical solutions that are closer to the true solution compared to other methods in most of the range. And figure 3 shows the real part of the numerical solutions for example 5.1, with different noise levels. From this figure, it is known that the proposed numerical solution is a stable approximation of the exact solution. Table 1 shows errors of the four regularization methods and the iteration numbers k of the Landweber iterative method for different noise level in example 5.1. We can see that the errors will decrease as the noise level. The results show that the Landweber iterative method will give the best approximation and the Moore-Penrose method will give the worst result in this example.

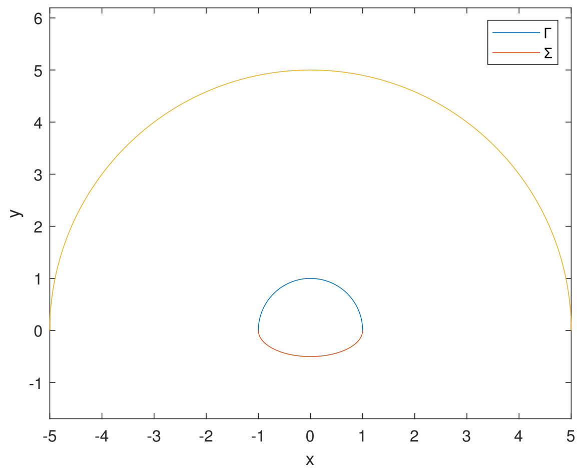

FIGURE 1. The boundary curves Γ, Σ and virtual boundary ∂B in example 5.1.

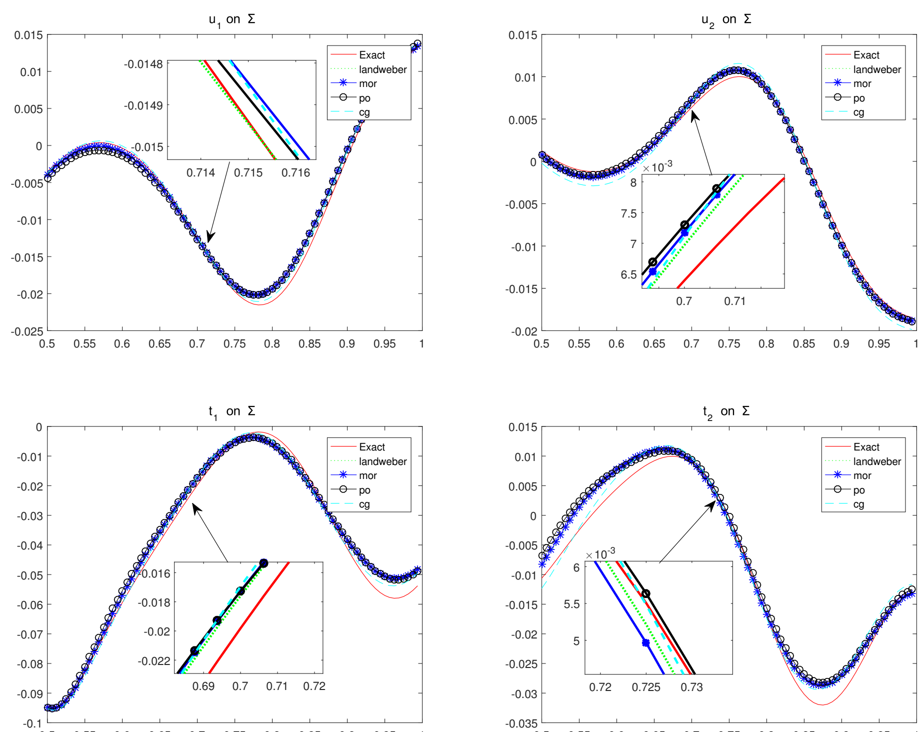

FIGURE 2. The numerical solution and the true solution on Σ obtained using different methods under the error level of 0.1 in example 5.1.

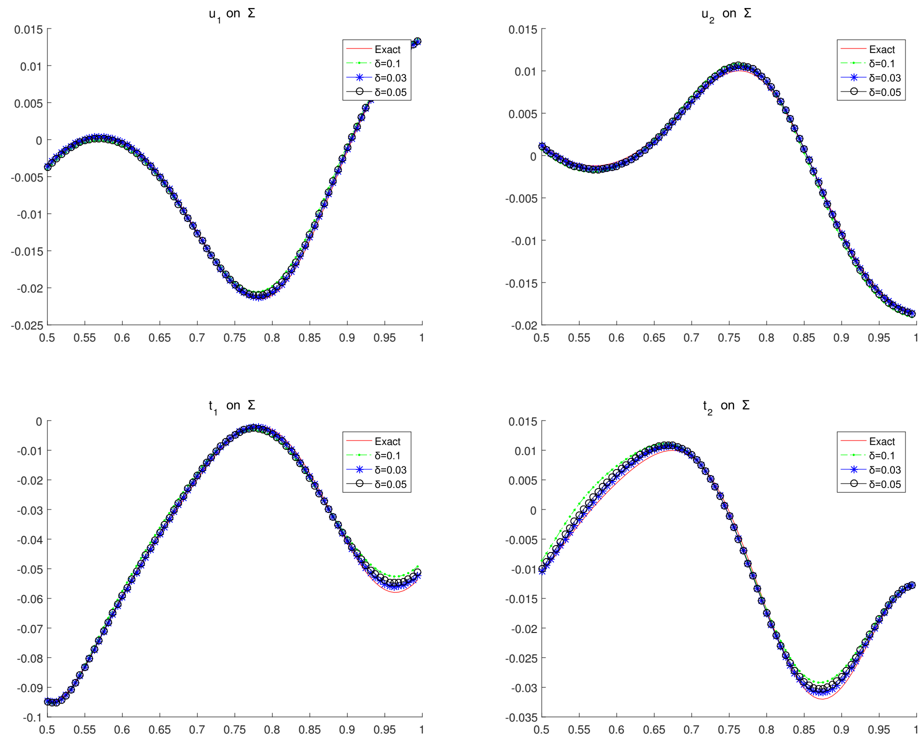

FIGURE 3. The exact solution and the numerical solution on Σ with different noise levels in example 5.1.

TABLE 1. Solution errors of four regularization methods and the iteration numbers k of the Landweber iterative method for different noise levels in example 5.1

Noise Level	Moore-Penrose	CG	regularization	Landweber	iterations
0.3	0.4493993993	0.1746680954	0.1648413373	0.1585650958	18
0.2	0.2267597014	0.1377902612	0.1160873539	0.1263513181	36
0.1	0.1839350743	0.0877108214	0.0698267237	0.0763326733	134
0.05	0.0898867329	0.0519252895	0.0493794180	0.0436510521	566
0.03	0.0428777569	0.0338485096	0.0425175091	0.0288131876	1926
0.01	0.0284685366	0.0143286332	0.0370841194	0.0123241872	17955

Example 5.2. Consider the exact solution on a doubly connected domain is the same as in Example 5.1. The known part boundary is given by $\Gamma = (\cos t, 2\sin t)$, $t \in [0, 2\pi]$, and the missing part of the boundary is $\Sigma = (0.25\cos t, 0.4\sin t - 0.3\sin^2 t)$, $t \in [0, 2\pi]$. In this example,we choose $\partial B = (25\cos t, 25\sin t)$, $t \in [0, 2\pi]$ and investigate the case $\omega = 3, \lambda = \mu = 1$.

We choose the discrete points $N = 160$ of boundary Γ and the discrete points $M = 80$ on virtual boundary. Figure 4 shows the solution domain,Figure 5 shows the numerical solutions obtained by different methods and the exact solution for Example 2 when the noise level is $\delta = 0.1\,\|\boldsymbol{b}\|$. It can be observed that the improved Landweber iteration method provides numerical solutions that are closer to the true solution compared to other methods in most of the range. And figure 6 shows the real part of the numerical solutions for example 5.2, with different noise levels. From this figure, it is known that the proposed numerical solution is a stable approximation of the exact solution. Table 2 shows errors of the three regularization methods and the iteration numbers k of the Landweber iterative method for different noise level in example 5.2. We can see that the errors will decrease as the noise level. The results show that the Landweber method will give the best approximation.

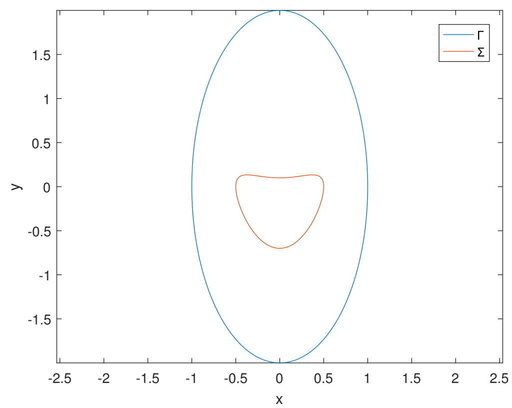

FIGURE 4. The boundary curves Γ, Σ in example 5.2.

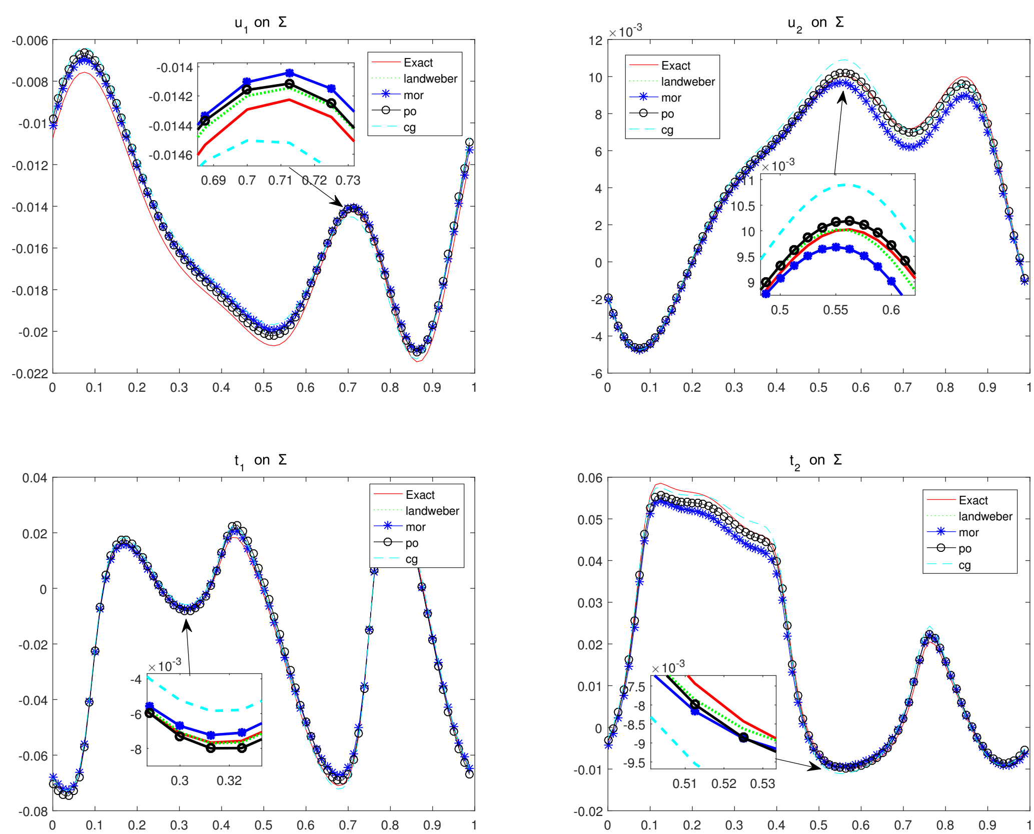

FIGURE 5. The numerical solution and the true solution on Σ obtained using different methods under the error level of 0.1 in example 5.2.

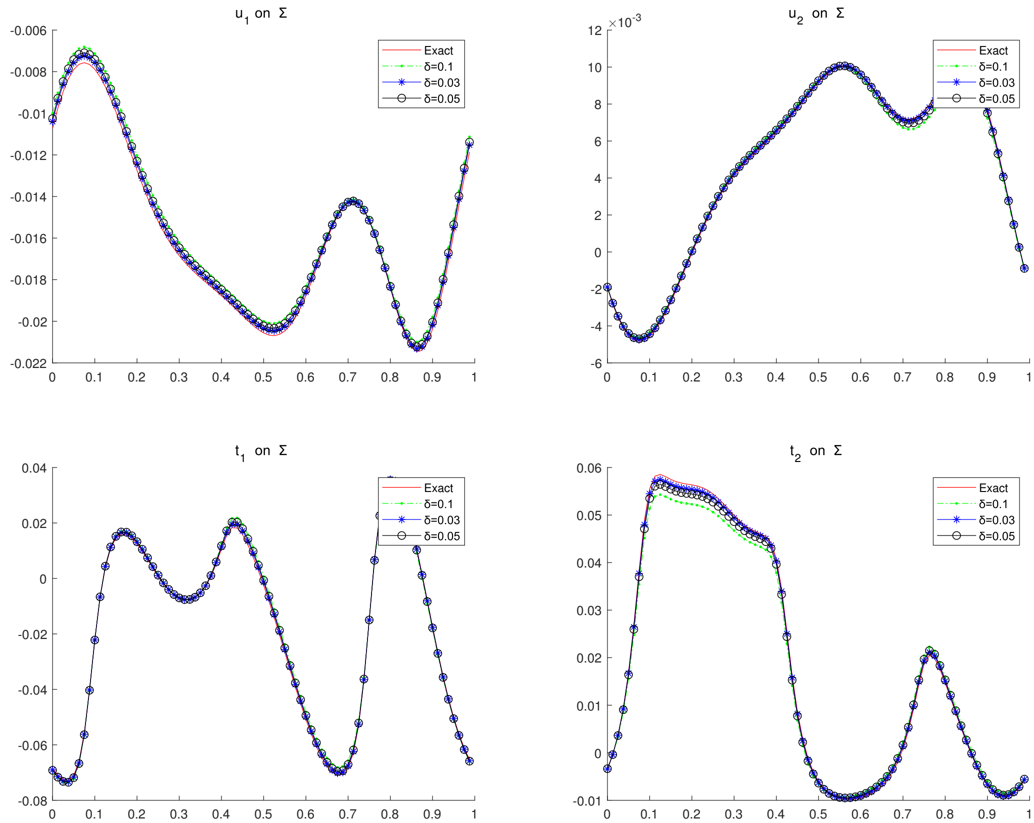

FIGURE 6. The exact solution and the numerical solutions on Σ with different noise levels in example 5.2.

TABLE 2. Solution errors of three regularization methods and the iteration numbers k of the Landweber iterative method for different noise levels in example 5.2

Noise Level	Moore-Penrose	CG	regularization	Landweber	iterations
0.3	0.1421495412	0.1055258000	0.1705895446	0.1236391390	5
0.2	0.0891481767	0.0791264824	0.1205944501	0.0847829919	8
0.1	0.0419615751	0.0580590997	0.0611995929	0.0426234395	22
0.05	0.0222060718	0.0525248548	0.0278202252	0.0204922798	72
0.03	0.0140453998	0.0553005362	0.0151060049	0.0118445396	195
0.01	0.0052344923	0.0549088173	0.0053952254	0.0050705450	1961

6. CONCLUSION

The aim of this study is to investigate the Cauchy problem of the Navier equations on a two-dimensional plane. Firstly, we formulate the Navier equations along with the given Dirichlet boundary conditions and Neumann boundary conditions. Based on the fundamental solution of the Navier equations, it is discretized into a ill-conditioned system of linear equations. We then consider the perturbed equation system $\boldsymbol{A}\boldsymbol{\varphi}^{\delta} = \boldsymbol{b}^{\delta}$. Initially, we employ the pseudoinverse method to solve this ill-conditioned system of linear equations and discuss the ill-posedness of the system by introducing SVD. We further solve the ill-posed linear equation system by truncating the SVD and analyze the construction of regularization operators using filtering functions. Next, we present the Tikhonov regularization method based on the Morozov discrepancy principle and provide several strategies for seeking regularization parameters in both prior and posterior settings. We also briefly introduce the conjugate gradient method. Lastly, we introduce the Landweber iteration method and demonstrate its regularization nature by finding its filtering function. We prove its convergence and divergence properties. Based on this, we combine it with the Tikhonov regularization method and propose an improved Landweber iteration method. By adjusting the initial value of the iteration and controlling the number of iterations, we can improve the accuracy of the numerical solution. We ensure the stability of the numerical solution by discussing two cases of noisy data simultaneously. Finally, we present numerical examples on a simply connected domain and a doubly connected domain. We compare the numerical solutions under different error levels and demonstrate that the improved Landweber iteration method can stably obtain the numerical solution. By comparing the differences between the numerical solutions obtained by different methods and the true solution, we verify that this method has higher accuracy compared to other methods.

Statements and Declarations

The authors declare that they have no conflict of interest, and the manuscript has no associated data.

References

[1] G. Alessandrini, L. Rondi, E. Rosset, and S. Vessella. The stability for the Cauchy problem for elliptic equations. Inverse Problems, 25(12):123004, 2009.
[2] A. P. Calderon. Uniquess in the Cauchy problem for partial differential equations. American Journal of Mathematics, 80:16-36, 1958.
[3] V. Isakov. Inverse Problems for Partial Differential Equations. Springer-Verlag, New York, 1998.
[4] L. Marin, L. Elliott, D. B. Ingham, and D. Lesnic. Boundary element method for the Cauchy problem in linear elasticity. Engineering Analysis with Boundary Elements, 25:783-793, 2005.
[5] L. Marin, L. Elliott, D. B. Ingham, and D. Lesnic. Boundary element regularization methods for solving the Cauchy problem in linear elasticity. Inverse Problems in Engineering, 10:335-357, 2002.
[6] L. Comino, L. Marin, and R. Gallego. An alternating iterative algorithm for the Cauchy problem in anisotropic elasticity. Engineering Analysis with Boundary Elements,31:667-682, 2007.
[7] F. Delvare, A. Cimetière, J. L. Hanus, and P. Bailly. An iterative method for the Cauchy problem in linear elasticity with fading regularization effect. Computer Methods in Applied Mechanics and Engineering, 199:3336-3344, 2010.
[8] B. Durand, F. Delvare, and P. Bailly. Numerical solution of Cauchy problem in linear elasticity in axisymmetric situations. International Journal of Solids and Structures, 48:3041-3053, 2011.
[9] L. Marin, L. Elliott, D. B. Ingham, and D. Lesnic. An iterative boundary element algorithm for a singular Cauchy problem in linear elasticity. Computational Mechanics, 28:479-488, 2002.
[10] L. Marin and B. T. Johansson. Relaxation procedures for an iterative MFS algorithm for the stable reconstruction of elastic fields from Cauchy data in two-dimensional isotropic linear elasticity. International Journal of Solids and Structures, 47:3462-3479, 2010.
[11] L. Marin and B. T. Johansson. A relaxation method of an alternating iterative algorithm for the Cauchy problem in linear isotropic elasticity. Computer Methods in Applied Mechanics and Engineering, 199:3179-3196, 2010.
[12] E. Turco. An effective algorithm for reconstructing boundary conditions in elastic solids. Computer Methods in Applied Mechanics and Engineering, 190:3819-3829, 2001.
[13] L. Marin and D. Lesnic. Boundary element solution for the Cauchy problem in linear elasticity using singular value decomposition. Computer Methods in Applied Mechanics and Engineering, 191:3257-3270, 2002.
[14] L. Marin and D. Lesnic. Regularized boundary element solution for an inverse boundary value problem in linear elasticity. Communications in Numerical Methods in Engineering, 18:817-825, 2002.
[15] L. Marin and D. Lesnic. Boundary element-Landweber method for the Cauchy problem in linear elasticity. IMA Journal of Applied Mathematics, 70:323-340, 2005,.
[16] L. Marin and D. Lesnic. The method of fundamental solutions for the Cauchy problem in twodimensional linear elasticity. International Journal of Solids and Structures, 41:3425-3438, 2004.
[17] L. Marin, D. N. Hào, and D. Lesnic. Conjugate gradient-boundary element method for the Cauchy problem in elasticity. Quarterly Journal of Mechanics and Applied Mathematics, 55:227-247, 2002.

[18] E. Turco. A boundary elements approach to identify static boundary conditions in elastic solids from stresses at internal points. Inverse Problems in Engineering, 7:309-333, 1999.

[19] Y. Sun, D. Zhang, and F. Ma. A potential function method for Cauchy problem of elliptic operators. Journal of Mathematical Analysis and Applications, 395:164-174, 2012.

[20] Y. Sun, X. Lu, and B. Chen. The method of fundamental solutions for the high frequency acoustic-elastic problem and its relationship to a pure acoustic problem. Engineering Analysis with Boundary Elements, 156:299-310, 2023.

[21] N. Zabaras, V. Morellas, and D. Schnur. Spatially regularized solution of inverse elasticity problems using the BEM. Communications in Applied Numerical Methods, 5:547-553, 1989.

[22] A. Maniatty, N. Zabaras, and K. Stelson. Finite element analysis of some elasticity problems. Journal of Engineering Mechanics, 115:1303-1317, 1989.

[23] T. J. Martin, J. D. Halderman, and G. S. Dulikravich. An inverse method for finding unknown surface tractions and deformations in elastostatics. Computers and Structures, 56:825-835, 1995.

[24] D. S. Schnur and N. Zabaras. Finite element solution of two-dimensional elastic problems using spatial smoothing. International Journal for Numerical Methods in Engineering, 30:57-75, 1999.

[25] V. A. Kozlov, V. G. Maz'ya, and A. V. Fomin. An iterative method for solving the Cauchy problem for elliptic equations. Computational Mathematics and Mathematical Physics, 31:45-52, 1991.

[26] G. Fairweather and A. Karageorghis. The method of fundamental solutions for elliptic boundary value problems. Advances in Computational Mathematics, 9:69-95, 1998.

[27] Y. Sun and F. Ma. A meshless method for the Cauchy problem in linear elastodynamics. Applicable Analysis, 93:2647-2667, 2014.

[28] Y. Sun, F. Ma, and D. Zhang. An integral equations method combined minimum norm solution for 3D elastostatics Cauchy problem. Computer Methods in Applied Mechanics and Engineering, 271:231-252, 2014.

[29] R. Kress and W. Rundell. Nonlinear integral equations and the iterative solution for an inverse boundary value problem. Inverse problems, 21:1207-1223, 2005.

[30] N. S. Mera, L. Elliott, D. B. Ingham, and D. Lesnic. A comparison of different regularization methods for a Cauchy problem in anisotropic heat conduction. International Journal of Numerical Methods for Heat and Fluid Flow, 13:528-546, 2003.

[31] R. Kress. Linear Integral Equations. Springer, New York, 2nd edition, 1989.

[32] G. Fairweather and A. Karageorghis. The method of fundamental solutions for elliptic boundary value problems. Advances in Computational Mathematics, 9:69-95, 1998.

[33] X. Xiong, X. Cao, S. He, and J. Wen. A modified regularization method for a Cauchy problem for heat equation on a two-layer sphere domain. Applied Mathematics and Computation, 290:240-249, 2016.

[34] F. Cakoni, R. Kress, and C. Schuft. Integral equations for shape and impedance reconstruction in corrosion detection. Inverse Problems, 26:095012, 2010.

[35] I. Borachok, R. Chapko, and B. T. Johansson. An inverse elastodynamic data reconstruction problem. Journal of Engineering Mathematics, 134:3, 2022.

[36] R. Chapko, B. T. Johansson, and L. Mindrinos. On a boundary integral solution of a lateral planar Cauchy problem in elastodynamics. Journal of Computational and Applied Mathematics, 367:112463, 2020.